

# FEED WATER TEMPERATURE REGULATION IN A MARINE REGENERATIVE STEAM CYCLE

**M. Hanafi**

Marine Eng. & Naval Arch. Dept.,  
Faculty of Engineering, Alexandria University,  
Alexandria, Egypt.

**M. Mosleh**

Ship Engineering Dept.,  
Faculty of Engineering, Suez Canal Univ.,  
Port Said, Egypt.

## ABSTRACT

Dynamic energy balances for complex transient heat transfer process in closed type feed water heaters w.r.t. command and perturbations signals are presented. Digital computational assessment in parametric study of the dynamics of feed water temperature regulation is carried out. Stability problems encountered from large transportation lags and time delays as well as time and frequency domains analysis are investigated.

## NOMENCLATURE

A	Circumferential tube area subjected to heat transfer ( $m^2$ )		
$A_1$	Inside peripheral tube area per unit length for one tube ( $m^2/m$ )	$\bar{G}$	Boiler evaporation (kg/hr)
$A_2$	Outside peripheral tube area per unit length for one tube ( $m^2/m$ )	G(S)	Forward path transfer function
C	Total capacity of steam vapour in shell, tube wall and shell (KJ/K)	H(S)	Feedback path transfer function
$C_{sh}$	Thermal capacity of shell (KJ/K)	$h_1$	Inside film coefficient of heat transfer ( $KJ/m^2.s.K$ )
$C_v$	Thermal capacity of steam vapour in shell (KJ/K)	$h_2$	Outside film coefficient of heat transfer ( $KJ/m^2.s.K$ )
$C_w$	Thermal capacity of tube wall (KJ/K)	K	Sensor's gain (-)
$c_f$	Specific heat of feed water (KJ/kg.K)	$K_o$	Overall gain = $K_p.K_v/K$ (mm/K)
$c_{sh}$	Specific heat of shell (KJ/kg.K)	$K_p$	Controller's gain (mm/K)
$c_w$	Specific heat of tube wall (KJ/kg.K)	$K_v$	Control valve gain (-)
$d_i$	Inner tube diameter (m)	LMTD	Logarithmic mean temperature difference between condensing steam and feed water in heater ( $^{\circ}C$ )
$d_o$	Outer tube diameter (m)	$M_f$	Feed water mass per unit length per tube (kg/m)
$d_s$	Inner shell diameter (m)	$M_p$	Percentage maximum overshoot of feed water outlet temperature deviation (-)
$d_{so}$	Outer shell diameter (m)	$M_v$	Steam mass enclosed in shell (kg)
$F'$	Product of kg water per meter length per tube by its velocity = feed water rate (kg/s)	$M_w$	Mass of tube wall per unit length per tube (kg/m)
$\bar{F}$	Normal flow of feed water (kg)	n	Number of tubes of feed water heater (-)
$\bar{F}'$	Rate of normal of water (kg/s)	$P_b$	Bled steam pressure (Pa)
$F_m$	Mass flow rate of feed water per unit free area ( $kg/m^2$ hr)	r	$\Delta\bar{F}/\bar{F}$ (-)
$F_s$	Rate of bled steam flow (kg/s)	S	Laplace operator (1/s)
FWT	Feed water temperature inlet to the boiler ( $^{\circ}C$ )		

T	Dead time of sensor (s)
$T_1, T_2$ and $T_{12}$	delay times of heat transfer process (s)
t	time (s)
U	Overall heat transfer coefficient (KJ/m <sup>2</sup> .s.k)
$\bar{U}$	Normal steady state value of overall heat transfer coefficient (KJ/m <sup>2</sup> .s.k)
v	Feed water velocity through heat exchanger (m/s)
w	Specific weight of water (kN/m <sup>3</sup> )
X	Displacement of control valve (mm)
x	Length of feed water heater (m)
$\lambda$	Heat lost by steam during condensation (KJ/kg)
$\Delta \dots$	Change in ... (-)
$\rho_f$	Density of feed water (kg/m <sup>3</sup> )
$\rho_{sh}$	Density of shell metal (kg/m <sup>3</sup> )
$\rho_w$	Density of tube metal (kg/m <sup>3</sup> )
$\rho_s$	Density of steam enclosed in shell (kg/m <sup>3</sup> )
$\theta_b$	Bled steam saturation temperature in steady state (°C)
$\theta_f$	Dynamic feed water temperature outlet of heat exchanger (°C)
$\delta\theta_r$	Steady state temperature rise of feed water through heater (°C)
$\theta_s$	Steam saturation temperature (°C)
$\theta_w$	Dynamic tube metal temperature (°C)
$\tau$	Time delay in controller (s)
$\tau_d$	Time delay in sensor (s)
$\tau_1$	Dead time in the heat transfer process dynamics (s)
$\tau_v$	Time delay in control valve (s)
$\omega_\pi$	Phase cross-over frequency (rad/s)

## INTRODUCTION

One of the complex problems in analyzing the dynamics of control systems is the study of heat exchangers dynamics for temperature regulation.

The heat transfer problem incorporated in the process dynamics comprises a fluid temperature function not only in time but also in the length of heat exchanger; a matter which yields a transportation lag in the plant beside the inevitable transportation lag incorporated in the temperature sensor. In addition to the excessive time delays in both sensor and control valve, the thermal capacities of condensate, bled steam enclosed

in shell, tube walls and the shell, together with inside and outside film coefficients of heat transfer, the conductivity of tubes will result in considerable large time delays characterizing the dynamic behavior of the automatic control loop.

Moreover, the existence of multi-perturbations, namely the variation in the fluid temperature in the heat exchanger and the fluctuation of boiler load to meet the propulsion requirements results in adding a complicated complexity to the problem. Dynamic heat exchangers are extremely varied depending on whether compressible or incompressible fluids are inside or outside the tubes.

After establishing conventional heat transfer science [1], the evolution of the dynamic analysis of heat exchangers took place in the branch of process dynamics in chemical engineering.

Among the pioneer research workers in this field were Gould, Cohen, Campbell, Catheron, DeLees, Koppel and Fricke [2-9]. While [5,6,7] carried out experimental research work on different types of heat exchangers, theoretical mathematical studies were presented by the others.

Meanwhile, further advances were developed in this field by reputed scientists of mechanical and chemical engineering. Some of the most famous investigators in the domain of control of steam installations were Oppelt, Quack, Profos, Doležal, Varcop and Isern [10-23] to whom is attributed the merit of the progress achieved in the art of regulation of steam power plants components. Additional contributions, particularly in mathematical analysis of heat exchangers, are ascribed to Masubuchi and Yang [24,25].

The aim of this paper is a parametric study for the dynamic analysis of closed type feed water heaters. In reality, two sources of perturbation affect the control loop. The first one is the variation in feed water temperature inlet to the heat exchanger attributed to change in condenser vacuum caused by a transition in a ship's course from hot to rather cold regions or vice versa. The second external disturbance is originated from the change in amount of condensate passing through the heaters caused by boiler load variation to adapt to propulsion requirements. The discussion on the perturbation influences is beyond the scope of this study and a separate research should be dedicated to analyzing this control system when subjected to the aforementioned effectual external disturbances.

The regenerative steam cycle under discussion includes either two or three heaters corresponding to the standard marine feed water temperatures 115.5°C (240 °F) and 160°C (320°F) respectively. The concept of equal temperature rise distribution among the heaters is adopted. The analysis in this paper is restricted to the first low pressure closed type feed water heater-assumed a single pass heater-as an illustrative demonstration of the problem of feed water temperature regulation.

In order not to violate the validity of the linearized obtained model only slight variations in condenser vacuum and amount of condensate are assumed. The vacuum is changed from 0.0478 bar abs. (28" 1/2 Hg vacuum) to 0.0647 bar abs (28" Hg vacuum) due to regional environmental deviations in sea cooling water temperatures.

Part and overload boiler evaporations are considered 90% and 110% respectively of the normal load.

### DYNAMIC SYSTEM OF EQUATIONS

Considering the marine regenerative steam power plant shown in Figure (1), with the known control conventions indicated on each system, the temperature control system under discussion in this paper is the low pressure single pass closed type feed water heater

enclosed with the dotted line,

Control schemes often used for heat exchangers are demonstrated in Figure (2). The scheme adopted in this research is that shown in Figure (2-a). The pneumatic controller illustrated in Figure (3) and based on the flapper-nozzle concept with double seat valve and minor feedback having  $P_1$  control property is used [26]. A concise description of this control valve is as follows: The increase in feed water temperature outlet will cause the increase in gas temperature inside the bulb and consequently the increase of its pressure. This will lead to the expansion of Bourdon tube and the augmentation of the gap between the flapper and nozzle. The operating air pressure under the primary diaphragm will decrease pulling downwards the double seat valve decreasing the air leakage from vent. The control air pressure will increase and the steam valve operated by this air is partially closed. Concerning the minor feedback the air pressure under the feedback below will increase and the nozzle approaches the flapper plate diminishing the air gap, thus transforming the control property of the controller from  $I_0$  to  $P_1$ , whereas the bulb and its tube connection as temperature measuring device incorporates both dead and delay times.

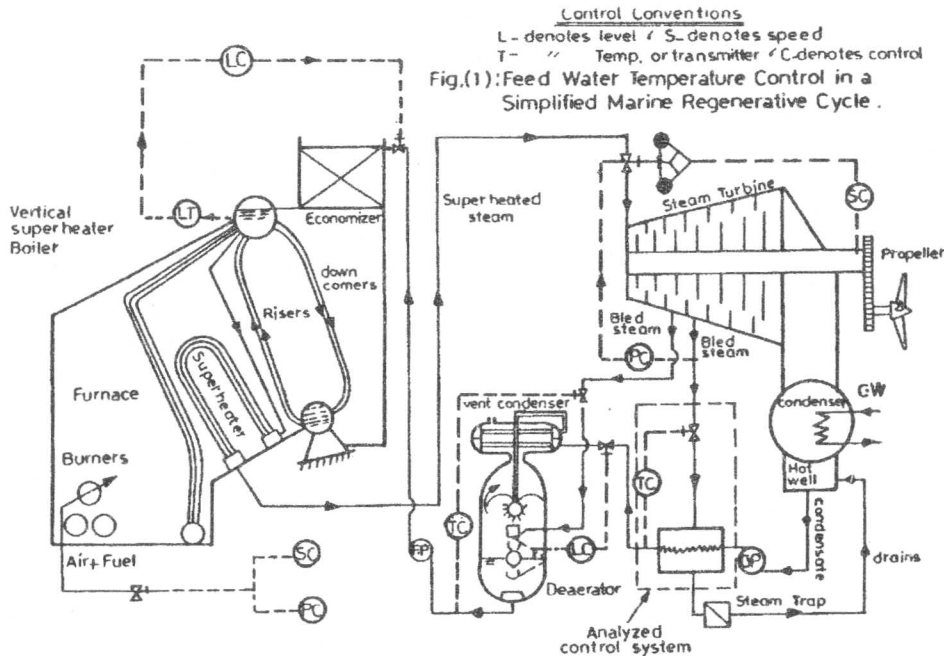


Figure 1. Feed water temperature control in a simplified marine regenerative cycle.

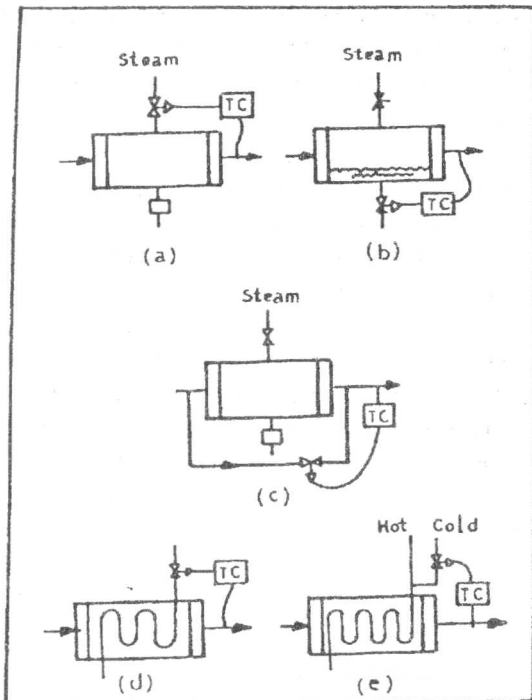


Figure 2. Control schemes for heat exchangers (a) throttle steam flow, (b) throttle condensate (c) bypass method, (d) throttle liquid flow (e) regulate inlet temperature.

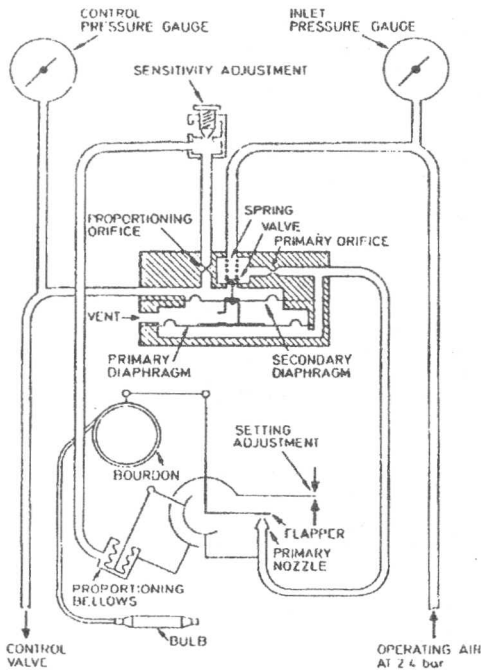


Figure 3. Pneumatic dialset controller.

Materials and dimensions of feed water heater discussion are illustrated in the schematic shown in Figure (4), [27].

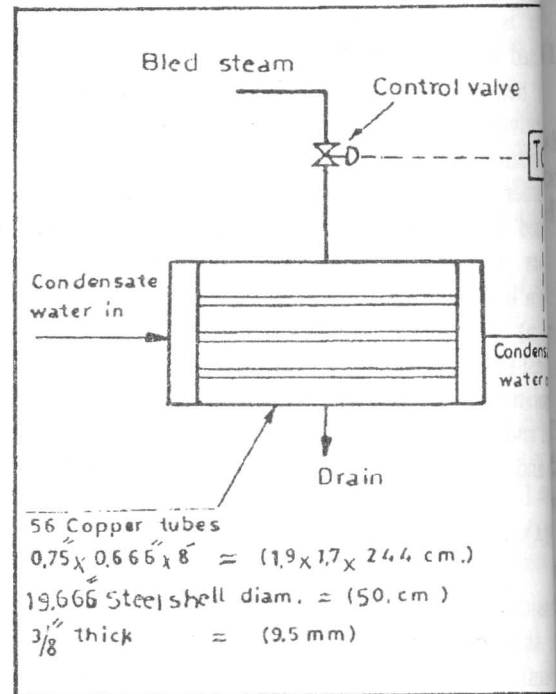


Figure 4. Dimensions of analyzed single-pass water heater.

Concerning the response to changes in temperature  $\theta_s$ , the usual steady state assumptions axial conduction, no backmixing, and constant properties are made. It is also necessary to assume wall resistance and no capacity in the condensate to limit the equations to second order. If significant the wall resistance could be split and added to the film resistances, and the condensate film capacity be added to that of the wall [27].

The water temperature  $\theta_f$  is a function in both time and tube length  $x$ , i.e:

$$\theta_f = \theta_f(t, x)$$

then

$$\Delta\theta_f = \left. \frac{\partial\theta_f}{\partial t} \right|_{x=\text{const.}} \cdot \Delta t + \left. \frac{\partial\theta_f}{\partial x} \right|_{t=\text{const.}} \cdot \Delta x$$

The energy balance for the water stream is written

for a length  $dx$  of a single tube:

Since the rate of heat added to the feed water equals the heat transferred through the tube wall temperature to the water it follows [27]:

$$M_f \cdot \frac{dx}{dt} \cdot c_f \cdot \Delta\theta_f = h_1 (A_1 \cdot dx) (\theta_w - \theta_f) \quad (3)$$

Substituting equation (2) in equation (3) it follows

$$M_f c_f \left(\frac{\partial \theta_f}{\partial t}\right) dx + F' \cdot c_f \cdot \frac{\partial \theta_f}{\partial x} dx = h_1 A_1 \cdot dx (\theta_w - \theta_f) \quad (4)$$

where

$$F' = M_f \cdot \frac{dx}{dt} = M_f \cdot v$$

In order to write the energy balance for the wall, the energy stored in the wall equals the difference between the heat transferred from the steam to the wall and the heat transferred from the wall to the feed water:

$$M_w c_w \left(\frac{\partial \theta_w}{\partial t}\right) dx = h_2 A_2 dx (\theta_s - \theta_w) - h_1 A_1 dx (\theta_w - \theta_f) \quad (5)$$

Introducing the following time constants to equations (4) and (5), it could be written

$$T_1 = \frac{M_f c_f}{h_1 A_1} = R_1 C_1,$$

$$T_2 = \frac{M_w c_w}{h_2 A_2} = R_2 C_2,$$

and

$$T_{12} = \frac{M_w c_w}{h_2 A_1} = R_1 C_2$$

where  $R_1$ ,  $R_2$ ,  $C_1$  and  $C_2$  denote thermal resistances and capacities. Equations (4) and (5) are reduced to:

$$T_1 \left(\frac{\partial \theta_f}{\partial t}\right) + v T_1 \left(\frac{\partial \theta_f}{\partial x}\right) = \theta_w - \theta_f \quad (6)$$

and

$$T_2 \left(\frac{\partial \theta_w}{\partial t}\right) = (\theta_s - \theta_w) - \frac{T_2}{T_{12}} (\theta_w - \theta_f) \quad (7)$$

According to [2,3,4], the partial differential equations (6) and (7) are converted to ordinary differential equations by taking the Laplace transform with respect to time.

The variables  $\theta_f$  and  $\theta_w$  in the following transformed equations represent deviations from the normal values at any point along the exchanger:

$$T_1 S \theta_f + v T_1 \left(\frac{d\theta_f}{dx}\right) = \theta_w - \theta_f \quad (8)$$

$$T_2 S \theta_w = \theta_s - \theta_w - \frac{T_2}{T_{12}} (\theta_w - \theta_f) \quad (9)$$

Eliminating  $\theta_w$  gives the first order equation namely:

$$\frac{v}{a} \left(\frac{d\theta_f}{dx}\right) + \theta_f = \frac{b}{a} \theta_s \quad (10)$$

$$\text{where } a = \frac{(T_1 S + 1)(T_{12} T_2 S + T_{12} + T_2) - T_2}{T_1 (T_{12} T_2 S + T_{12} + T_2)}$$

i.e.

$$a \approx a_1 S + a_0$$

resulting from the quotient of numerator by denominator of (a)

where  $a_1 = 1$

$$\text{and } \frac{b}{a} = \frac{1}{(T_1 T_2) S^2 + (T_1 + T_2 + T_1 T_2 / T_{12}) S + 1} \text{ or,}$$

$$\frac{b}{a} = \frac{1}{\alpha S^2 + \beta S + 1}$$

The solution of equation (10) for the boundary condition  $\theta_f = 0$  at  $x = 0$  is the step response of the first order system:

$$\frac{\theta_f}{\theta_s} = \frac{b}{a} (1 - e^{-ax/v}) \quad (11)$$

The term  $x/v = \tau_1$  is the time for water to flow through the tubes, which is the transportation lag. Hence:

$$\frac{\theta_f}{\theta_s} = \frac{1}{\alpha S^2 + \beta S + 1} [1 - e^{-(a_1 S + a_0)\tau_1}] \quad (12)$$

Bode plots of equation (12) have oscillatory nature particularly at the existence of large transportation lag [2,3,4,27].

To introduce the vapour capacity enclosed in shell, the tube wall and the shell capacity as well, the energy balance for the tubes and shell could be summarized as the difference between heat released from steam and the heat transferred to the feed water is stored in the tube wall shell and vapour capacities, i.e.

$$(C_v + C_w + C_{sh}) \frac{d\theta_s}{dt} = (K_v F_s \lambda) X - UA(\theta_s - \frac{\theta_{fi} + \theta_f}{2}) \quad (13)$$

where,

$$C_v = \frac{M_v}{P} \lambda \left( \frac{\partial P}{\partial \theta_s} \right),$$

$$M_v = \frac{\pi}{4} [d_s^2 - n \cdot d_o^2] (x) \cdot \rho_s \quad \text{and}$$

$P$  = The steam pressure in shell approximated to about 3/8 the bled steam pressure [27].

For initial feed water temperature  $\theta_{fi} = 0$ , the transformation of equation (13) to the Laplace domain yields:

$$(C S + UA) \theta_s = (K_v F_s \lambda) X + \frac{UA}{2} \theta_f \quad (14)$$

where,  $C = C_v + C_w + C_{sh}$

As discussed before, the transfer function of the sensor has the form:

$$\frac{K e^{-TS}}{1 + \tau_d S} \quad (15)$$

A transportation lag of 1 second is assumed due to the location of the sensor distant from the condensate outlet.

The reason for selecting a gain  $K$  is to reach error of about 2% and this gain should be numerically compensated in the forward path. The transfer function for the controller could be written as:

$$\frac{K_p}{1 + \tau S}$$

Assuming only friction forces in the control valve while neglecting its inertia forces, the transfer function relating the control valve to the control displacements is

$$\frac{1}{1 + \tau_v S}$$

Combining equations (12), (14), (15), (16) and results in the block diagram shown in Figure 1, indicating the transfer functions, unit step response and control properties of each minor block.

It is emphasized that in the following numerical computations the role of boiler load and inlet water temperature as external disturbances are discarded. Parametric analysis at different operating conditions will be dynamically considered. In this paper concerns the theoretical treatment of the control system response to a change in inlet condensate temperature. A constant steam temperature [27] could be deduced from equation (10) for  $\theta_s = 0$  and  $\theta_f = \theta_F = \text{constant} = 0$  as:

$$\theta_f = \theta_F \cdot e^{-(a_1 S + a_0)\tau_1}$$

or  $\theta_f = K_1 \cdot e^{-a_1 \tau_1 S}$

where  $K_1 = \theta_F \cdot e^{-a_0 \tau_1}$

Considering the response of the control system to changes in the amount of condensate water: If the flow is increased suddenly, there is an immediate change in the heat-transfer coefficient throughout the exchanger. However, the percentage change in the heat-transfer coefficient is less than the percentage increase in the flow rate and so the exit temperature must drop, and this disturbance spreads out over a time interval of roughly  $\tau_1$  seconds, the time for water to flow through the exchanger.

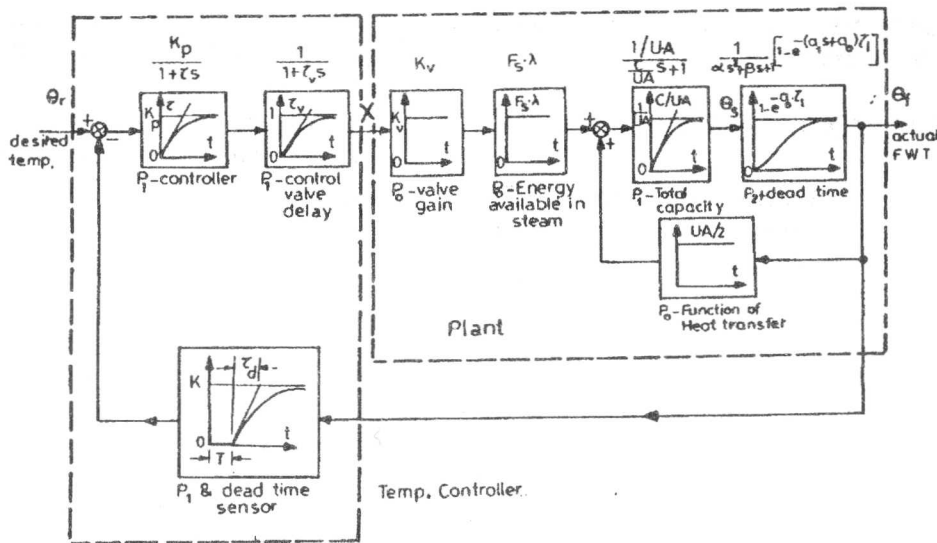


Figure 5. Block diagram for feed-water temperature regulation without disturbances.

If negligible wall capacity and a linearized relationship between the overall coefficient and the flow [8] are assumed,

then 
$$U = \bar{U}(1 + \beta_1 r)$$

where,  $r = \frac{\Delta \bar{F}}{\bar{F}}$  = change in flow / normal flow

The value of the factor  $\beta_1$  ranges between 0 and 0.8 depending on the fraction of the total resistance in the inside film.

The heat balance for the feed water is

$$M_f c_f \left( \frac{\partial \theta_f}{\partial t} \right) + \bar{F}' (1+r) c_f \left( \frac{\partial \theta_f}{\partial x} \right) = \bar{U} A (1 + \beta_1 r) (\theta_s - \theta_f) \quad (19)$$

$$\text{or } T' \left( \frac{\partial \theta_f}{\partial t} \right) + \bar{v} T' (1+r) \left( \frac{\partial \theta_f}{\partial x} \right) = (1 + \beta_1 r) (\theta_s - \theta_f) \quad (20)$$

where:  $\bar{v}$  is the normal velocity of water and

$T'$  is a time constant equals  $M_f c_f / \bar{U} \cdot A$ .

Since 
$$\theta_f = \bar{\theta}_f + \Delta \theta_f \quad (21)$$

where  $\bar{\theta}_f$  is a function of length and bearing in mind that the steam temperature is kept invariant i.e.  $\theta_s = \bar{\theta}_s$ . Substituting equation (21) into equation (20) gives,

$$T' \left( \frac{\partial \Delta \theta_f}{\partial t} \right) + \bar{v} T' (1+r) \left( \frac{\partial \bar{\theta}_f}{\partial x} + \frac{\partial \Delta \theta_f}{\partial x} \right) = (1 + \beta_1 r) (\bar{\theta}_s - \bar{\theta}_f - \Delta \theta_f) \quad (22)$$

Neglecting the terms  $r(\partial \Delta \theta_f / \partial x)$  and  $\beta_1 r \Delta \theta_f$  and taking the Laplace transform leads to

$$(T' S + 1) \Delta \theta_f + \bar{v} T' \left( \frac{d \Delta \theta_f}{dx} \right) + \bar{v} T' (1+r) \frac{d \bar{\theta}_f}{dx} = (1 + \beta_1 r) (\bar{\theta}_s - \bar{\theta}_f) \quad (23)$$

Using the steady-state relationship  $\bar{\theta}_s - \bar{\theta}_f = (\theta_s - \theta_{fi}) e^{-\tau_1/T}$ , we obtain:

$$(T' S + 1) \Delta \theta_f + \bar{v} T' \left( \frac{d \Delta \theta_f}{dx} \right) = -(\theta_s - \theta_{fi}) r (1 - \beta_1) e^{-\tau_1/T} \quad (24)$$

The solution for  $\Delta \theta_f = 0$  at  $x = 0$  is the transfer function for flow rate changes, i.e.

$$\frac{\Delta \theta_f}{r} = \frac{-(\bar{\theta}_s - \bar{\theta}_{fi}) (1 - \beta_1) e^{-\tau_1/T} (1 - e^{-\tau_1 s})}{T' S} \quad (25)$$

At the termination of the mathematical simulation, equations from (18) through (25) which represent the description of the response of the regulated feed water temperature to external disturbances of inlet feed water

temperature and boiler evaporation will not be considered in the digital solutions of this work.

THE DYNAMIC MODEL UNDER DISCUSSION

Referring to the block diagram illustrated in Figure (5), both the open and closed-loops transfer functions of the control system are deduced as:

O.L.T.F = G(s).H(s) =

$$\frac{(K.K_p.K_v.F_s.\lambda/UA).e^{-TS}[1-e^{-(a_1s+a_0)\tau_1}]}{(1+\tau S)(1+\tau_v S)(1+\tau_d S)\left\{\left(\frac{C}{UA}S+1\right)(\alpha S^2+\beta S+1)-\frac{1}{2}[1-e^{-(a_1s+a_0)\tau_1}]\right\}}$$

(26)

C.L.T.F. =  $\frac{G(s)}{1+G(s)H(s)}$  =

$$\frac{(K.K_p.K_v.F_s.\lambda/UA).(1+\tau_d S).[1-e^{-(a_1s+a_0)\tau_1}]}{(1+\tau S)(1+\tau_v S)(1+\tau_d S)\left\{\left(\frac{C}{UA}S+1\right)(\alpha S^2+\beta S+1)-\frac{1}{2}[1-e^{-(a_1s+a_0)\tau_1}]\right\}}$$

$$= \frac{1}{\frac{KK_pK_vF_s\lambda}{UA}.e^{-TS}[1-e^{-(a_1s+a_0)\tau_1}]}$$

(27)

It is to be noted that the transportation lag is expanded by the padé second approximation, i.e.

$$e^{-\mu s} \approx \frac{1-0.5\mu S+0.0833\mu^2 S^2}{1+0.5\mu S+0.0833\mu^2 S^2}$$

(28)

where  $\mu$  is any value denoting dead time. After hard mathematical manipulations equations (26) is transformed to a quotient of fourth degree polynomial in S divided by tenth degree polynomial, while equation (27) is transformed to a quotient of fifth degree polynomial in S over tenth degree polynomial.

NUMERICAL DATA PROCESSED:

- The invariant data is:
- Boiler pressure 41 bar (615 psia)
- Boiler saturation temperature = 251.5 °C (485 °F)
- Superheated steam temperature = 454 °C (850 °F)
- Dryness fraction of vapour in shell  $\kappa$  is assumed 0.88.
- Vapour Volume in shell is computed as 0.40 m<sup>3</sup>
- $\rho_w$  = 8835 kg/m<sup>3</sup>
- $\rho_{sh}$  = 8005.3428 kg/m<sup>3</sup>
- $c_w$  = 0.3936 KJ/kg.K

- $c_f$  = 4.187 KJ/kg.K
- $c_{sh}$  = 0.4606 KJ/kg.K
- $C_w$  = 28.6926 KJ/K
- $C_{sh}$  = 138.6841 KJ/K
- $h_2$  = 31677 KJ/m<sup>2</sup>. hr. K
- $K_p$  = 3.5 mm/K
- $K_v$  = 0.05 (-)
- $K$  = 0.4562 (-)
- $\tau$  = 0.3 s
- $\tau_v$  = 3 s
- $\tau_d$  = 6 s
- $T$  = 1 s
- $a_1$  = 1 (-)

Feed water temperature entering the boiler are 110 (240 °F) in case of two feed water heaters and 120 (320 °F) when three heaters are used. temperature rise per heater is assumed.

Condenser vacuum is assumed to be 0.0478 bar (28" 1/2 Hg vacuum) and 0.0647 bar abs. (29" Vacuum).

Bled steam saturation temperature is assumed 2.78 °C (5 °F) higher than that of the condenser outlet.

Normal boiler evaporation (100% load) is taken as 27200 kg/hr ( $\approx$  60000 lb/hr) with variations ranging from 90% and 110% of the normal load.

Table (1) indicates the remainder of the numerical data depending on the variations in feed water temperature, condenser vacuum and boiler evaporation.

An illustration of the detailed calculation is demonstrated in the appendix applied to case (1).

RESULTS AND DISCUSSION

The transient response of only the plant which is surrounded by dotted lines in Figure (5) is displayed in Figure (6) for case (1). The temperature deviation is characterized by the influence of dead time, slow rate of response, very large steady state error reaching 100% and no oscillations. Knowing, the transfer function of the plant is

$$\frac{\theta_f(S)}{X(S)} = \frac{(K_v F_s \lambda / UA)[1 - e^{-(a_1 S + a_0)\tau_1}]}{\left(\frac{C}{UA} S + 1\right)(\alpha S^2 + \beta S + 1) - \frac{1}{2}[1 - e^{-(a_1 S + a_0)\tau_1}]}$$

Despite the seemingly acceptable response of the plant particularly after modifying the static error, the existence of two external disturbances renders the automatic loop unavoidable.



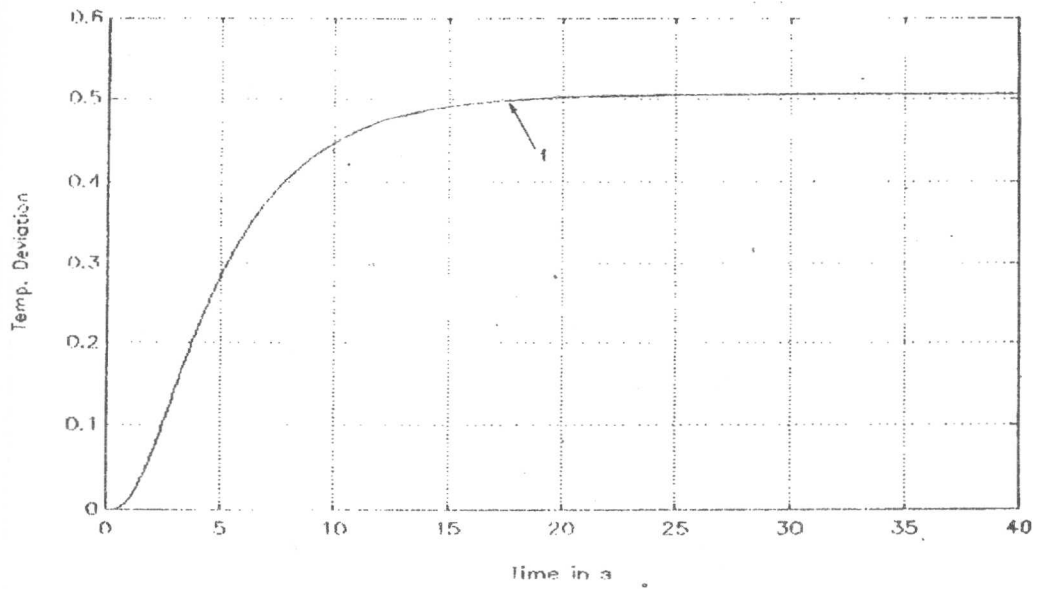


Figure 6. Transient response of the plant.

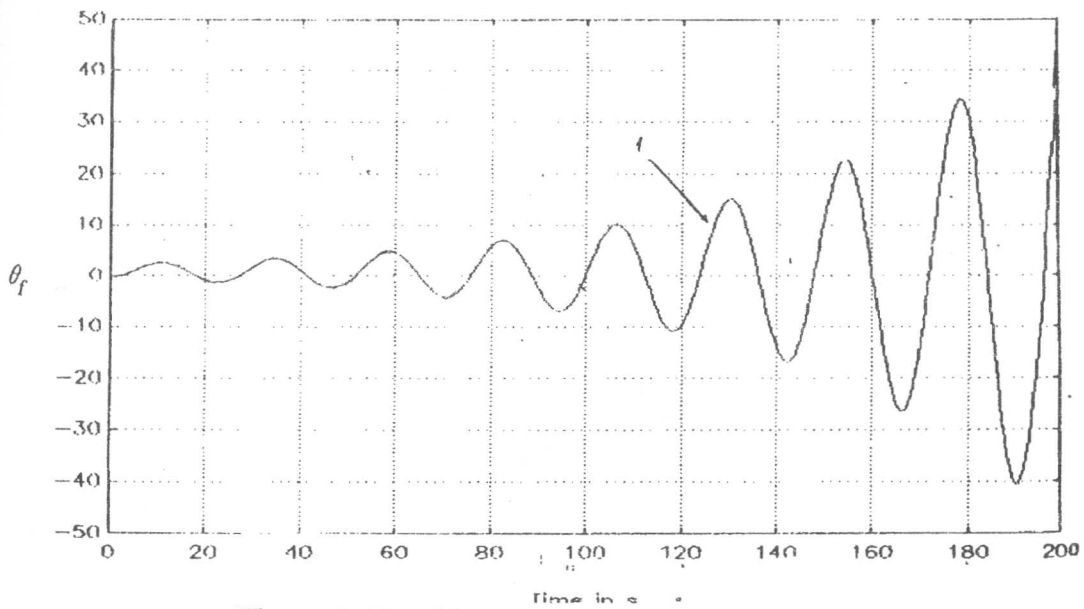


Figure 7. Unstable response of G.L ( $k_p, k_v = 0.4$ ).

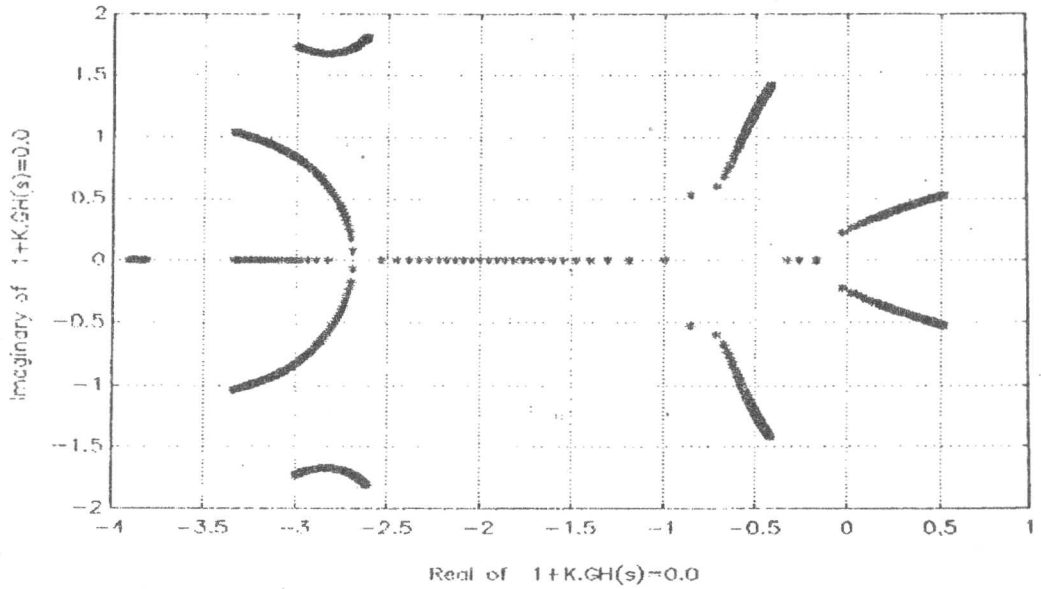


Figure 8. Root locus illustration ( $K=0$  ---  $25$ , Case 1).

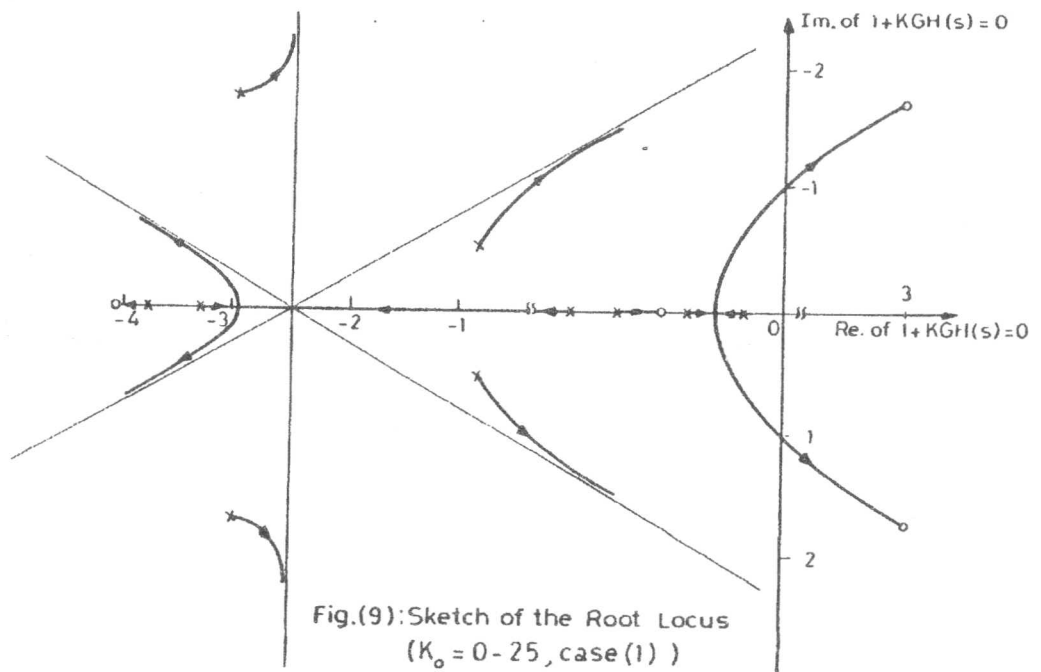


Fig.(9): Sketch of the Root Locus ( $K_0 = 0 - 25$ , case (1) )

Figure 9. Sketch of the root locus ( $k_0=0 - 25$ , Case (1)).

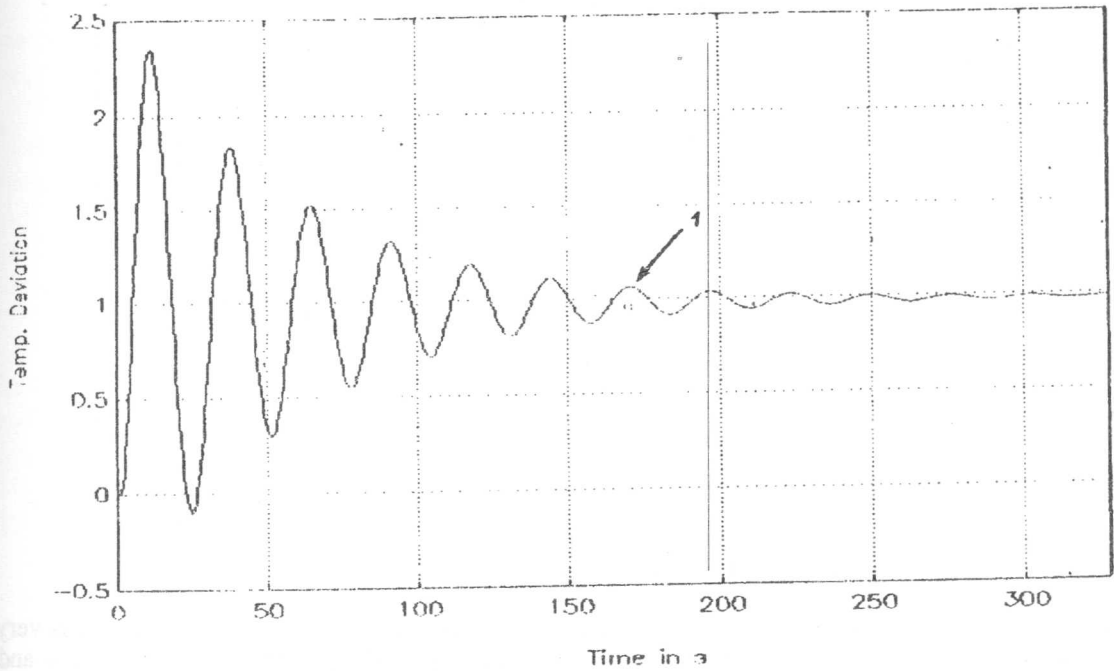


Figure 10. Transient response of C.L. ( $k_p k_v = 0.3425$ ).

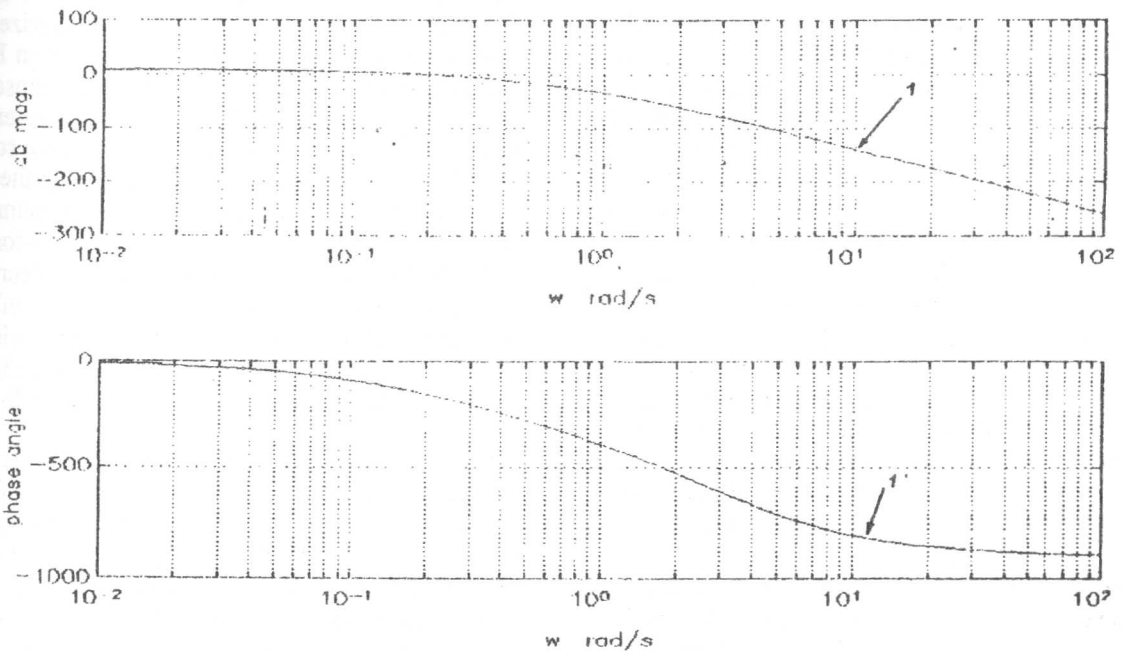


Figure 11-a. Bode plots of O.L. ( $k_p k_v = 0.3425$ ).

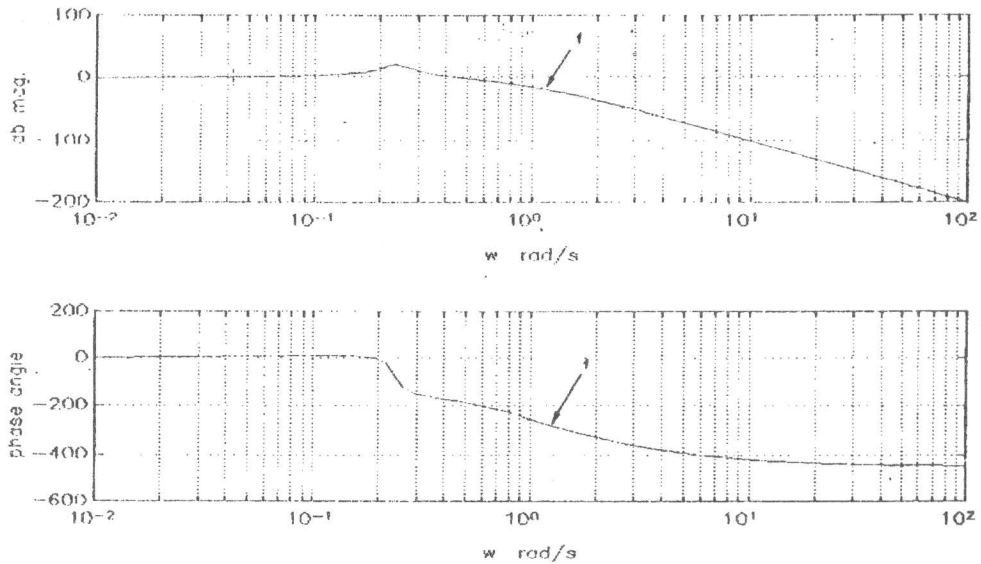


Figure 11-b. Bode plots of C.L. ( $k_p k_v = 0.3425$ ,  $k = 0.73$ ).

As preliminary exploration of the influence of the gains of the loop, the closed system proved to be unstable for case (1) when these values were selected:  $K_p K_v = 0.4$  and  $K = 1$ .

Two of the ten eigenvalues of the system are located in the right hand side of the complex plane. Detailed investigation of the stability of the closed loop is to establish the pole-zero mapping and plot the root locus of Evans by the aid of the open-loop transfer function  $K_o \cdot G \cdot H (S)$  in terms of the overall gain  $K_o = K_p \cdot K_v \cdot K$ . The root locus configuration printed by the computer for case (1) and  $K_o$  ranging from 0 to 25 is shown in Figure (8). The Figure displays that the stability border of case (1) is close to  $K = 1$  and  $K_p \cdot K_v = 0.3$ . A more clarifying hand sketch of the root locus indicated in Figure (8) is presented in Figure (9). Extensive investigations of the stability problem of the closed loop by Routh criterion certifies that the border of stability for the twelve cases lies in the neighborhood of  $K_p \cdot K_v = 0.25$  and  $K = 1$ . Should the value of  $K$  be reduced below 1 in order to get a reasonable steady state error approaching 0.02, while keeping the closed loop transfer function unchangeable, this implies dividing  $K_p \cdot K_v$  by  $K$ .

The influences of the gains  $K_p$ ,  $K_v$  and  $K$  on both the transient response of the C.L to a unit step input and the frequency response of the O.L are displayed in Figures (10), (11-a,b), (12) and (13) for case (1).

Provided with the product  $K \cdot K_p \cdot K_v = 0.3425$  and ( $K = \frac{1}{1.37} = 0.73$ ,  $K_p \cdot K_v = 0.25$ ), Figure (10) illustrates the transient response of the C.L. The system posses a low damping factor with oscillatory

overshoots; the maximum overshoot is very excessive (135%) while the settling times for 2% and 4% errors approaches 300 and 240 seconds respectively. The open loop Bode plots of the preceding case shown in Figure (11-a); corresponding gain and phase margins are 3.85 db & 27° respectively. Closed loop Bode plots for this case, with characterized resonance peak at  $\omega = 0.23$  rad/s are also shown in Figure (11-b). When the product  $K \cdot K_p \cdot K_v$  was chosen as 0.3425 with  $K = 0.5263$ ,  $K_p \cdot K_v = 0.1$  the transient response obtained for case (1). Figure (12) shows a considerable growth in the damping factor decreasing the number of oscillations and reducing both the maximum overshoot from 135% to 46% and the settling time-for 4% steady state error-from 240 to 70 seconds. A little decrease in speed of response is noticed too. In a similar manner to Figure (11), the O.L polar plot with the mentioned data is indicated in Figure (13) revealing gain and phase margins reaching 10.1db and 27° respectively.

This leads to the fact that reducing both  $K_p \cdot K_v$  and  $K$  improves the relative stability of this control system.

The final established selection of the gains is as follows:  $K_p = 3.5$ ,  $K_v = 0.05$  and  $K = 0.4562$ . With the exception of the maximum overshoot percentage which ranges from 30.5% to 48.5%, the chosen values of the gains  $K$ ,  $K_p$  and  $K_v$  match with the requirements of absolute and relative stability, time and frequency domain specifications. Since the objective of the paper is a control analysis and not a design problem, a parametric study will be carried on with the above mentioned values and the obtained results are demonstrated in Figures (14) through (28).

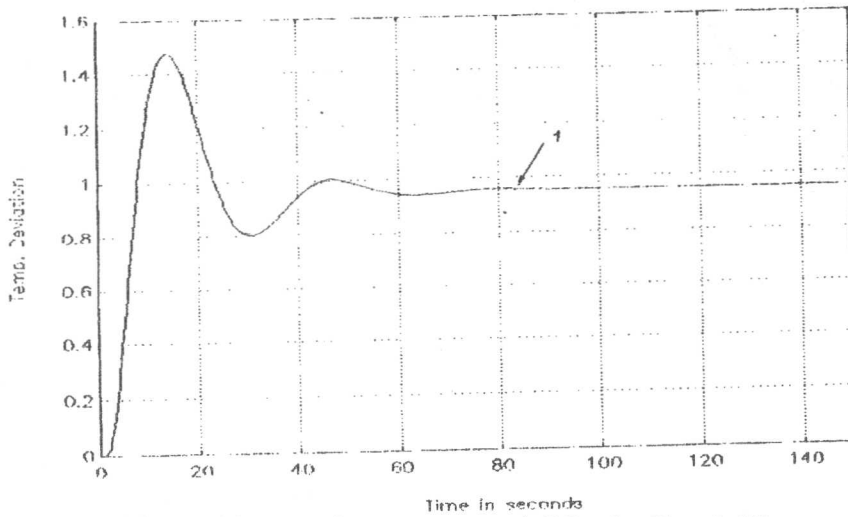


Figure 12. Transient response of C.L. ( $k_p K_v=0.19$ ).

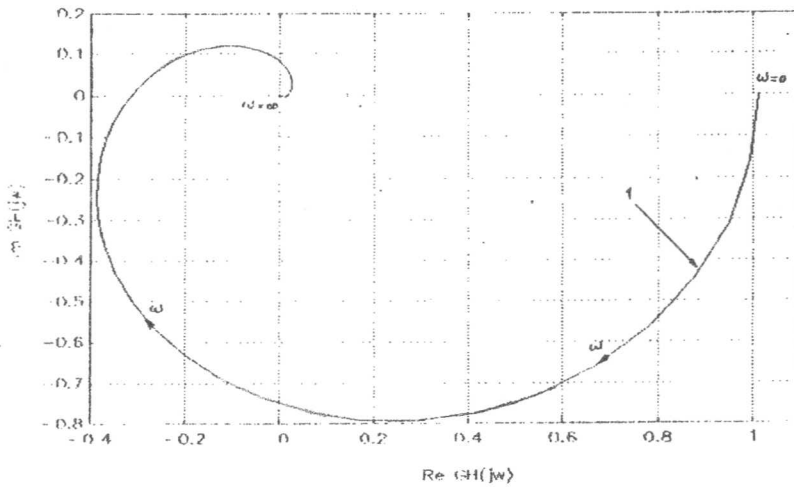


Figure 13. Polar plot ( $k_p k_v=0.19$ ).

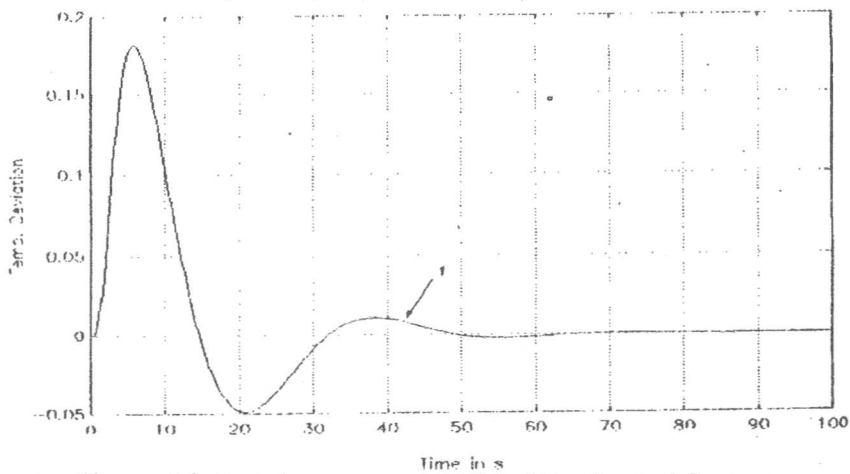


Figure 14. Impulse response of the C.L. Control System.

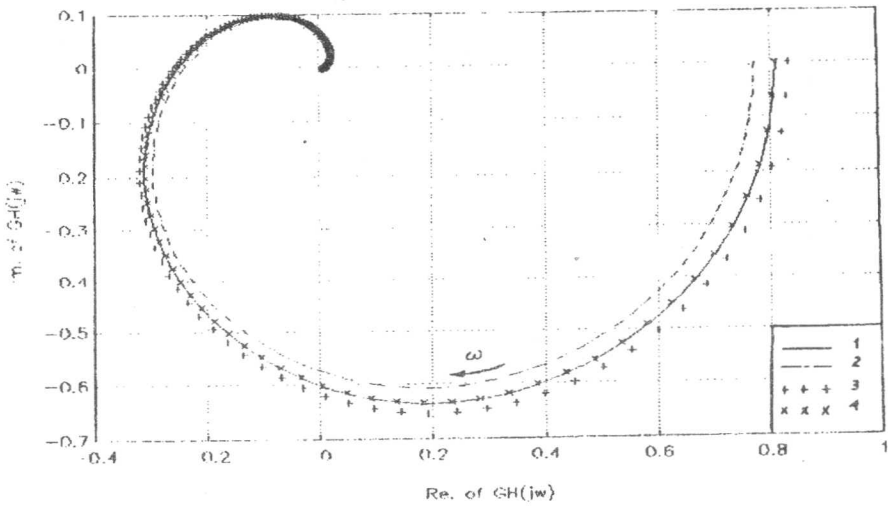


Figure 15. Effect of F.W.T. & Vacuum on polar plot.

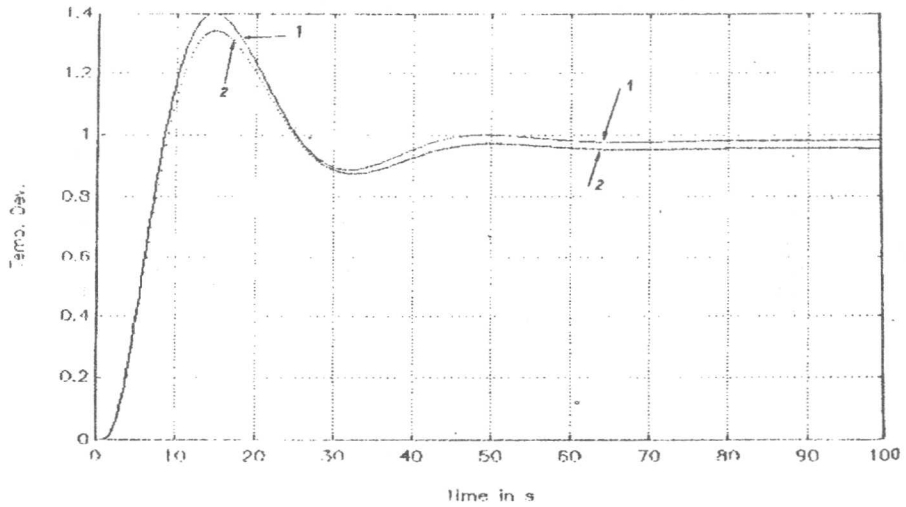


Figure 17. Effect of Vacuum variation.

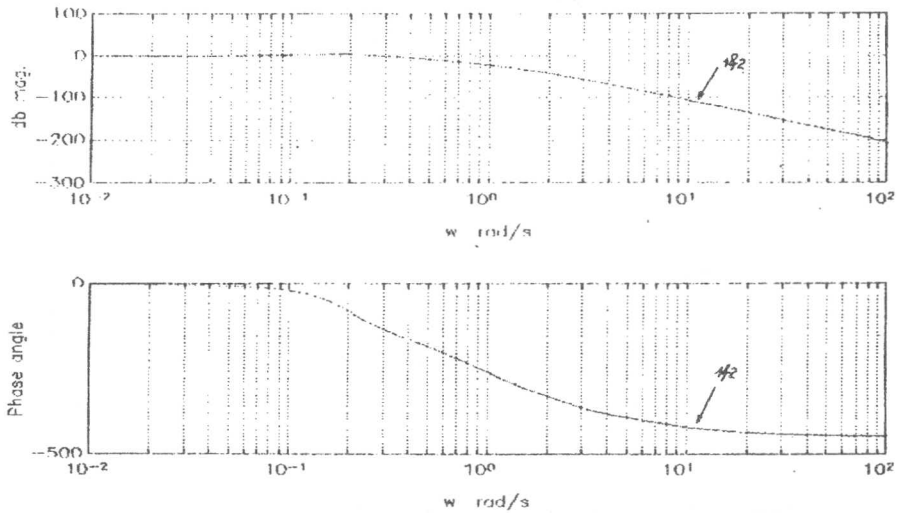


Figure 17. Bode plots of C.L. ( $k_p k_v = 0.1754$ ).

Figure (14) illustrates the impulse response of the C.L control system for case (1). The observed maximum overshoot is only 18% and the settling times for  $\pm 5\%$  and  $\pm 2\%$  of the final steady state value are 20 and 35 seconds respectively.

Before discussing the parametric analysis of the feed water temperature regulation, it is not surprising to find that the C.L transients of the twelve case studies are characterized by the narrow range (or even the constant value, e.g. the delay time) occupied by the delay, rise, peak and settling times beside the speed of response. To summarize these ranges:

Delay time is almost constant and equals 5.53 s

Rise time ranges from 4.9-5.75 s

Speed of response (after the dead time effect)  $\approx$  tangent ( $80^\circ - 81^\circ$ ) = 5.6713 - 6.3138

Peak time = 13.4 - 15.32 s

Settling time = 47 - 64.26 s (for 2% static error).

Limited variations in condenser vacuum and boiler load whereas dependence of F.W.T on the number of feed water heaters incorporated into the steam cycle give reason to the narrowness of the preceding ranges.

A relative stability comparison-displayed in polar plots between the first four case studies is shown in Figure (15).

A reduction of the vacuum from 0.0478 bar abs (28" Hg vacuum) to 0.0647 bar abs (28" Hg vacuum) at 100% boiler load and invariant F.W.T =  $115.5^\circ\text{C}$  raises the gain margin from 3.9636 to 4.1536 and reduces the phase cross over frequency  $\omega_\pi$  from 0.2507 to 0.2496 rad/s.

Adversely raising the F.W.T from  $115.5^\circ\text{C}$  to  $160^\circ\text{C}$  with the associated increase in number of heaters from 2 to 3 at 100% boiler evaporation and fixed vacuum of 0.0478 bar abs reduces the gain margin from 3.9636 to 3.8457 and increases  $\omega_\pi$  from 0.2507 to 0.2517 rad/s.

The same phenomena hold good when comparing case studies 1 & 3 and 2 & 4. It is worth mentioning that through the whole range of the parametric analysis of the case studies, the phase margins (and gain cross over frequencies) are undefined due to the non-intersection of the unit circle with the polar plots.

The effect of vacuum variation at fixed load and feed water temperature in time domain is indicated in Figure (16). Decreasing the vacuum, decreases the maximum overshoot and increases the static error.

On the other hand, the effect of vacuum variation on the closed loop in the frequency domain is negligible,

Figure (17). The system is characterized by a large bandwidth and no existence of resonant peak. Likewise, Figures (18) and (19) represent identical phenomena to Figures (16) and (17) respectively, but at different values of feed water temperatures.

It can be concluded that a change in condenser vacuum by 0.017 bar abs ( $\approx 1/2$ " Hg Vacuum) produces a change in the peak value ranging from 3.8% to 5.5% and a change in the settling time reaching from 1.3% to 2.2% respectively. In what concerns the effect of feed water temperature at constant boiler load and vacuum on the transients of the closed-loop, cases (1) & (3) and (2) & (4) are compared in Figures (20) and (21) respectively. Lowering the feed water temperature, lowers the maximum overshoot but increases the static error.

Similar changes approaching those values got from the change in condenser vacuum are obtained when varying the feed water temperature from  $115.5^\circ\text{C}$  to  $160^\circ\text{C}$  ( $240^\circ\text{F}$  to  $320^\circ\text{F}$ ) while increasing the number of heaters from 2 to 3. The dependence of feed water temperature inlet to the boiler on the number of heaters gives reason to its limited effect on the condensate outlet temperature deviation.

An emphatic conclusion is that the closed loop frequency response in Bode forms are exactly typical of the Bode plots shown in Figure (19). Therefore, additional repeated graphs will not be attached to avoid monotony. The influence of boiler load variation at fixed feed water temperature and vacuum on open-loop in db-magnitude versus phase angle plots are shown for cases (1), (5) and (9) in Figure (22). While the phase margins are undefined, minute changes in gain margins exist and will be displayed later.

Boiler part, normal and overloads effects on the transient response of the closed-loop are illustrated in Figure (23). Reducing the boiler load increases both the maximum overshoot and peak time beside decreasing the static error. A 10% increase or decrease in boiler load shifts the peak value from 3.7% to 5% and changes the settling time by 2.5% approximately. This effect when discussed on Bode plots of closed-loop Figure (24) shows intangible deviation on the db-magnitude plot and a slight variation on the phase angle plot.

Similar to closed-loop Bode plots of the twelve case studies, the plots have a distinguishing property of wide band width and no resonant peak.

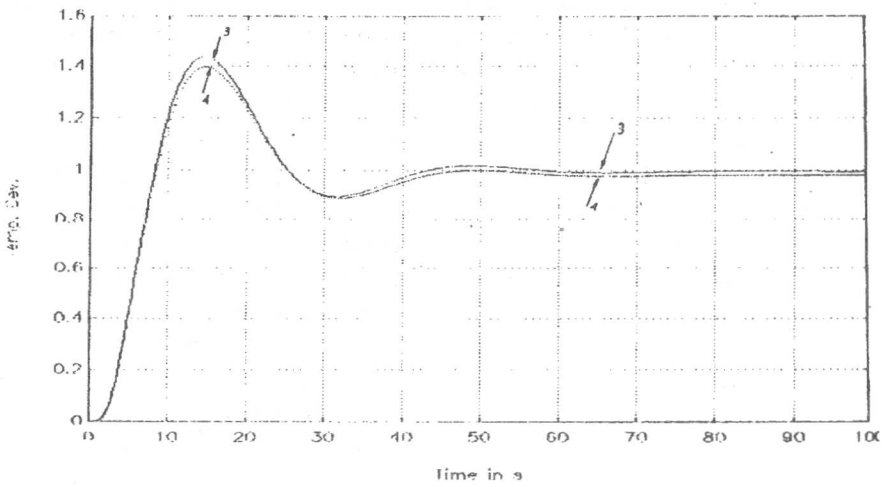


Figure 18. Effect of Vacuum variation.

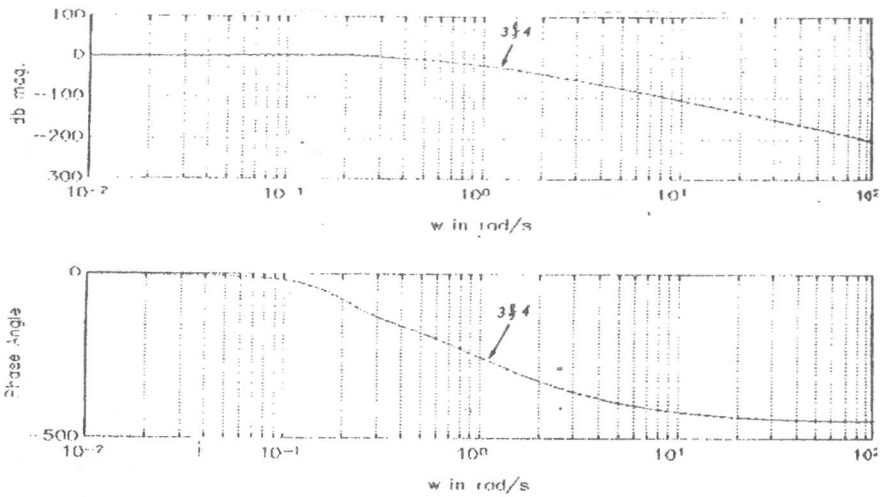


Figure 19. Effect of Vacuum variation on Bode plots of C.L.

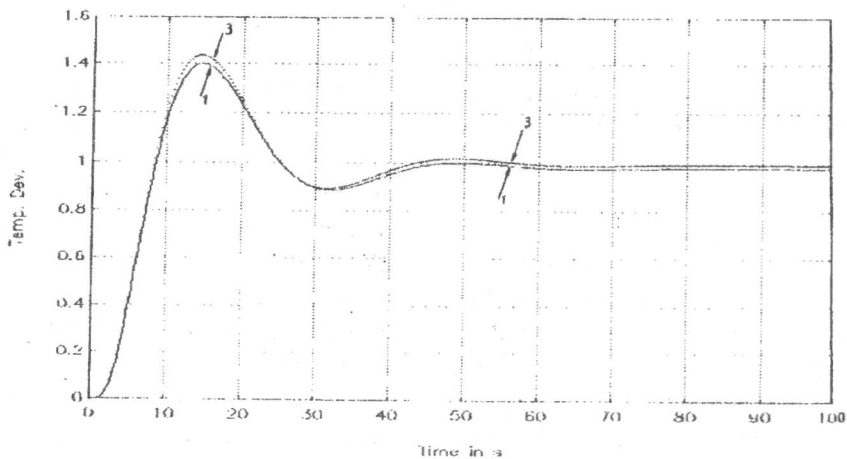


Figure 20. Effect of F.W.T.



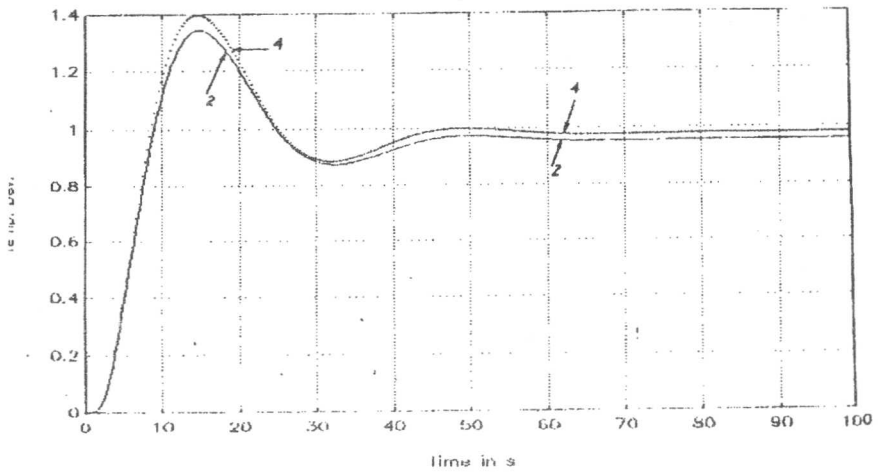


Figure 21. Effect of F.W.T.

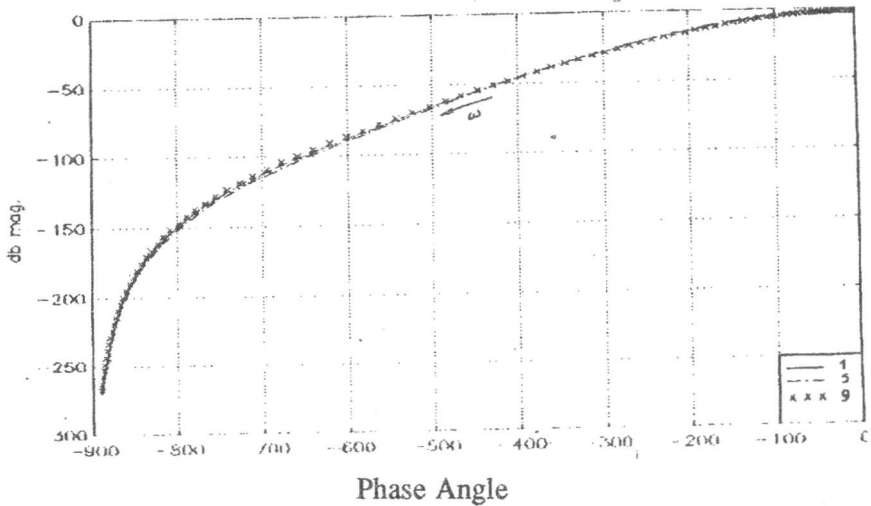


Figure 22. Effect of boiler load variation on db mag.-phase angle plot.

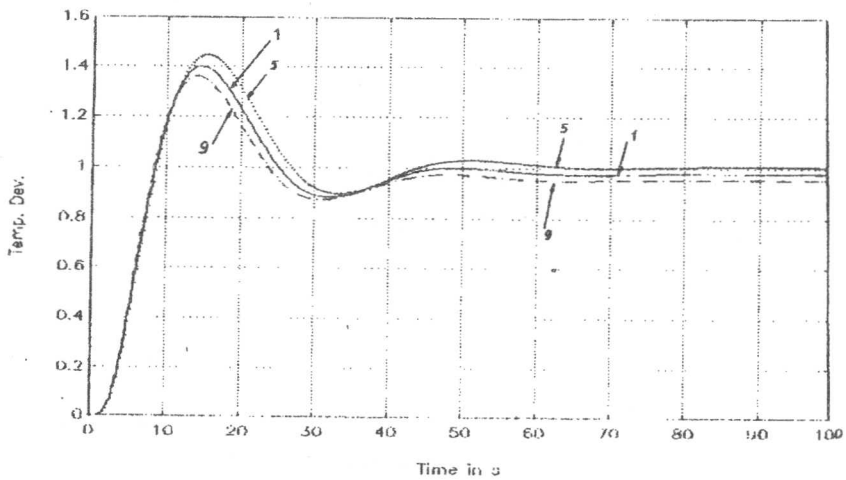


Figure 23. Effect of boiler load.

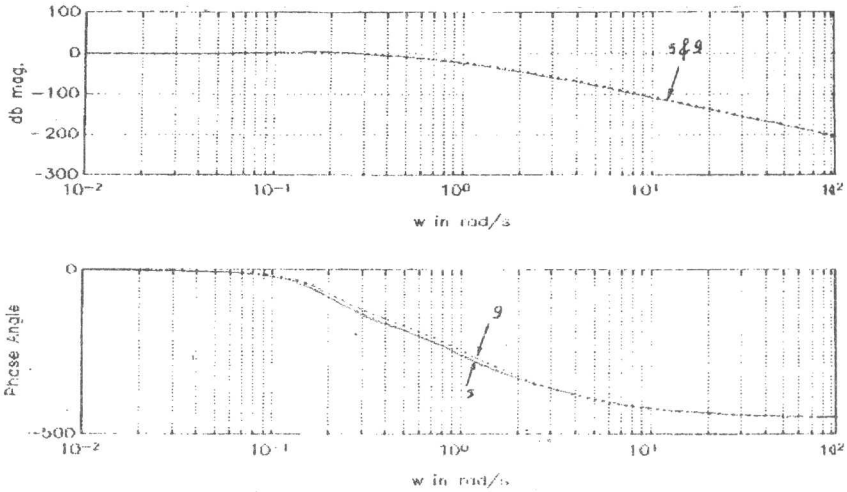


Figure 24. Effect of boiler load variation on Bode pots of G.L.

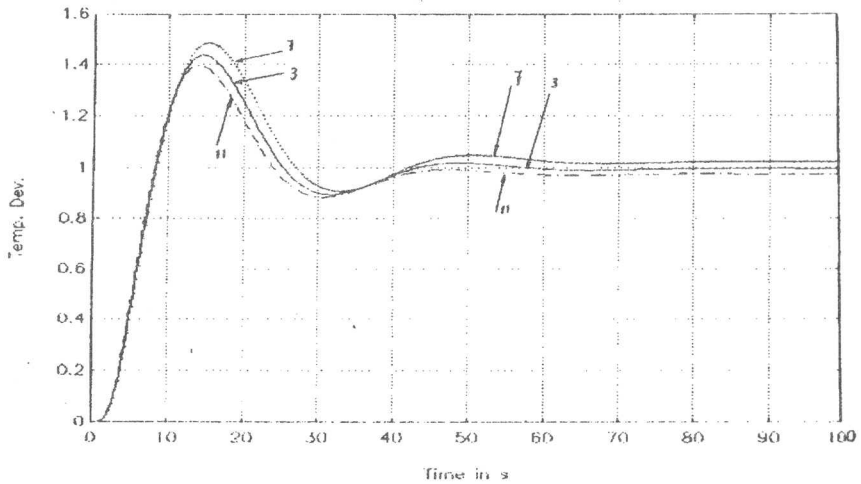


Figure 25. Effect of boiler load variation.

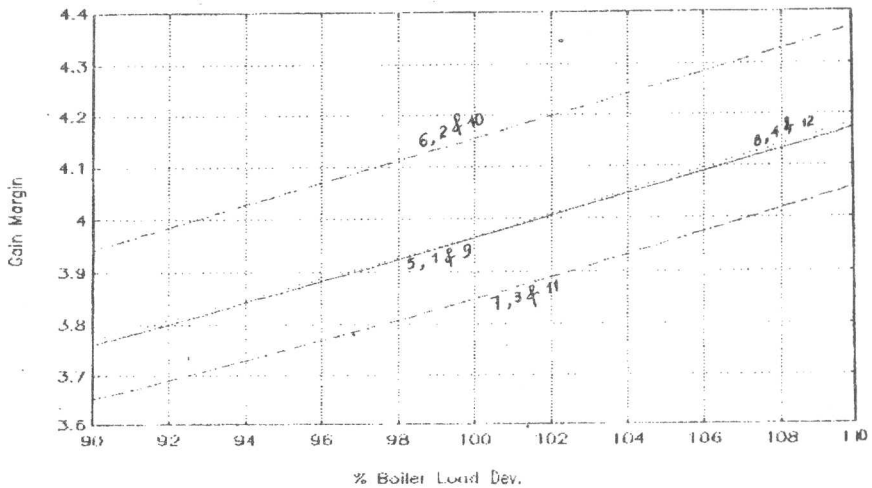


Figure 26. Variation of Gain Margin w.r.t. Control system parameters.

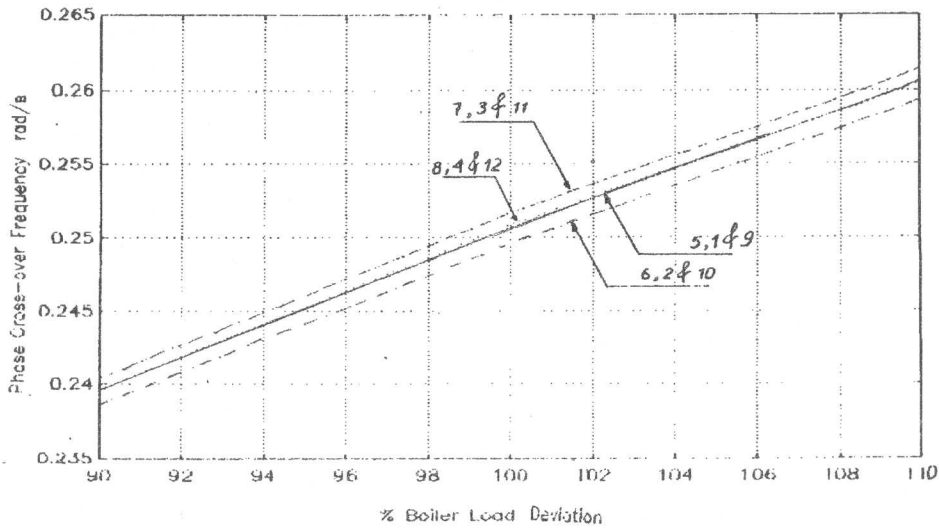


Figure 27. Variation of  $\omega_{\pi}$  w.r.t. Control system parameters.

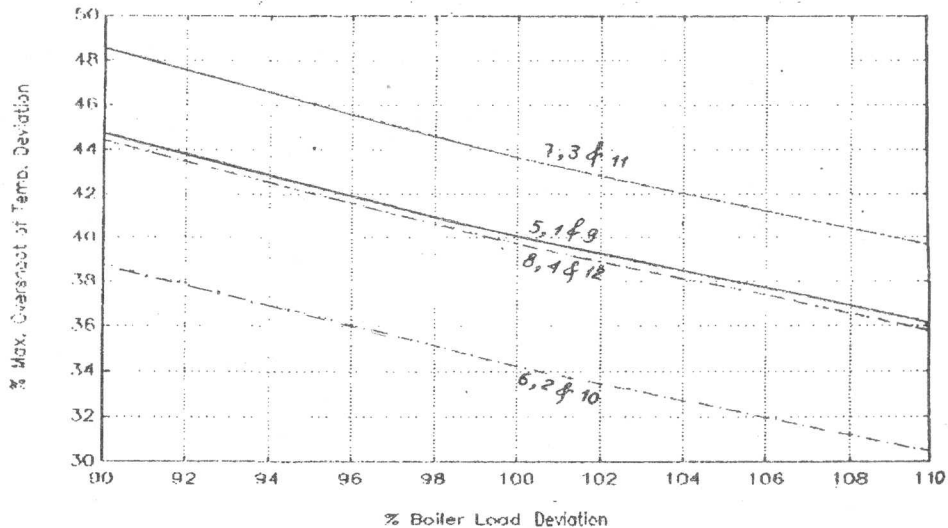


Figure 28. Variation of  $M_p$  w.r.t. Control system parameters.

Boiler load effect is discussed too in time domain for cases (3), (7) and (11) for feed water temperature equals  $160^{\circ}\text{C}$  and condenser vacuum equals 0.0478 bar abs. (28" 1/2 Hg vacuum). The concluded tendency for Figure (25) is identical to that shown in Figure (23).

The influence of control system parameters on gain margin, phase crossover frequency  $\omega_{\pi}$  and maximum overshoot  $M_p$  are plotted in Figures (26), (27) and (28) respectively. Figure (26) reveals that the gain margin is increased by raising the boiler load, decreasing the condenser vacuum and lowering the feed water temperature. Extreme values of gain margin are 3.6531 and 4.372.

From Figure (27), it is evident that, while  $\omega_{\pi}$  increases with the increase of boiler load, in contrast to gain margin,  $\omega_{\pi}$  decreases by lowering the vacuum and reducing the feed water temperature. Maximum and minimum values of  $\omega_{\pi}$  are 0.2614 and 0.2386 rad/s.

Lastly, the percentage maximum overshoot  $M_p$  which is displayed in Figure (28)- decreases with the increase of boiler load, the decrease of condenser vacuum and the reduction of feed water temperature. The lowest and highest observed values of  $M_p$  are 30.47% and 48.52%.

Programs for this study [28,29] had been executed in the Lloyd's computer laboratory at the department of

Marine Engineering and Naval Architecture, Alexandria University on the DELL-466/ME apparatus.

## CONCLUSION

Dynamic models for feed water temperature regulation w.r.t. command and perturbation signals of fluctuating boiler load or condenser vacuum have been presented.

Computational verification of the first model has been executed in extensive parametric analysis of the control loop. Major attention was paid to various values of condenser vacuum, boiler evaporation and required feed water temperature inlet to the boiler which depends on the number of feed water heaters. Each parameter affects the complex dynamics of heat transfer with the associated transportation lag and time delay owing to the resulting variations in bleed steam pressure, amount and heat content beside occurring changes in heat transfer coefficients and thermal capacities. The role played by the loop on absolute and relative stability has been scanned. The problem has been thoroughly analyzed in both time and frequency domains displaying which specifications are obtained and how far these are affected by the control system parameters.

The automatic loop dynamics proves insensitivity to slight deviations in system parameters.

## REFERENCES

- [1] Mc Adams, W.H., *Heat Transmission*, 3<sup>rd</sup> ed., McGraw-Hill Book Company, New York, 1954.
- [2] Gould, L.A., *The Dynamic Behaviour and Control of Heat Transfer Processes*, Sc. D. Thesis, Massachusetts Institute of Technology, 1953.
- [3] Cohen, W.C. and Johnson, E.F., *Dynamic Characteristics of Double-Pipe Heat Exchangers*, Ind. Eng. Chem., 48: 1031, 1956.
- [4] Campbell, D.P. *Process Dynamics*, John Wiley & Sons. Inc., New York, 1958.
- [5] Catheron, A.R., Goodhue S.H. and Hansen, P.D., *Control of Shell- and- Tube Heat Exchangers*, Trans. ASME Paper 59-IRD-14.
- [6] De Bolt, R.R., *Dynamic Characteristics Steam-Water Heat Exchanger*, M.Sc. Th. University of California, 1954.
- [7] Less, S. and Hougen, J.O., *Pulse Test Model Heat Exchange Process*, Ind. Eng. Chem., 48: 1064, 1956.
- [8] Koppel, L.B., *Dynamics of a Flow-Film Heat Exchanger*, I and EC Fundamentals 1:131, 1962.
- [9] Fricke, L.H., Morris, H.J., Otto, R.E. Williams T. J., *Process Dynamics and Analysis Computer Simulations of Shell-and-Tube Heat Exchangers*, Chem. Eng. Progr. Symposium Ser., 56 (31): 80, 1960.
- [10] Oppelt, W. *Kleines Handbuch technischer Vorgänge*, Verlag Chemie, 1954.
- [11] Quack, *Boilers with Load Regulation in National Economy*, Techn. Mitt, 5, pp. 193, 1957.
- [12] Quack, *Automation in the Steam Power Plant*, Techn. Mitt. Essen 50, 5, 1957.
- [13] Profos, P. *Control of Steam Installation*, Springer-Verlag, 1962.
- [14] Profos, P. *Load-Dependent Adjustment of Controller Setting for Superheater Temperature Control*.
- [15] Profos P. *The Dynamic Behaviour of Flow Evaporators with Uneven Temperature Distribution*, Regelungstechnik 13, pp. 57, 1965.
- [16] Profos, P., *Consideration of Future Control problems in Steam Generating Power Stations*, Mitt. VGB, 109, pp. 224-232, 1967.
- [17] Doležal, R., *Some Constructional Steps for Improvement of the Dynamic Characteristics of Steam Generators*, Seminaire International l' IBRA Bruxelles, 1966.
- [18] Doležal, R. & Varcop, L., *Process Dynamics Chapter (19). The Dynamic Characteristics of the Economizer*, Elsevier Publishing Company Ltd, Amsterdam, 1970.
- [19] Varcop, L. *The Various Modes of Operation of a Heat Exchanger*, Wärme, 71, pp. 121-126, 1965.
- [20] Varcop, L. *The Dynamics of Forced Flow Evaporator Systems under Consideration of Pressure Variations of the Evaporated Fluid*, Regelungstechnik, 15, pp. 404-412, 1967.

[21] Varcop, L., *Dynamics of the Evaporation Zone of an Evaporator with Unidimensional Flow*, Rozpravy Ceskoslovenske akademie ved, 77, 1967.

[22] Varcop, L. *On the Feedwater Supply and Fuel Flow Control in Once-Through Boilers*, IFAC Symposium On Multivariable Control Systems, 7/8 October Dusseldorf, 1968.

[23] Isermann, R., *The Determination of the Control Quality of Steam Temperature Control in Drum Boilers using an Analogue Computer Parts I and II*, Regelungstechnik, 10, pp. 469-475 and 11, pp. 519-522. 1966.

[24] Masubuchi, M., *Dynamic Response and Control of Multipass Heat Exchangers*, Trans. ASME J. Basic Eng., 820:51, 1960.

[25] Yang, W. & Masubuchi, M., *Dynamics for Process and System Control*, Chapter (5), *Dynamic Behaviour of Distributed Systems*, Gordon & Breach Science Publishers, New York, 1970.

[26] Jackson, L. & Embleton, W., *Instrumentation and Control Systems*, Reed's Marine Engg. Series, Thomas Reed Publications, London, 2<sup>nd</sup> Edition, 1975.

[27] Harriott, P., *Process Control*, Chapter (11)- *The Dynamics and Control of Heat Exchangers* McGraw-Hill Publishing Company, New York, 1977.

[28] Melsa, J., *Computer Programs for Computational Assistance in the Study of Linear Control Theory*, McGraw-Hill Book Company, 1973.

[29] \_\_\_\_\_ *MATLAB, The Mathworks Incorporation*, Stanford, 1986.

[30] Mikheyev, M., *Fundamentals of Heat Transfer*, Peace Publishers, Moscow, 1965, Appendix, Table A-19, pp. 369.

Appendix

Brief Sample of Analysis of Procedure

Normal boiler load = 27200 kg/hr ( $\approx$  60000 lb/hr)  
 Feed water temperature 115.5 °C (240 °F)  
 Condenser vacuum 0.0478 bar abs. (28 1/2" Hg)  
 Dimensions of heat exchanger 50 cm ( $\approx$  19.666")  
 Outer steel shell diameter with 9.5 mm ( $\approx$  3/8") thickness.  
 Dimensions of tubes are:

$d_i = 1.6916$  cm ( $\approx$  0.666")  
 $d_o = 1.905$  cm ( $\approx$  0.75")  $x = 244$  cm ( $\approx$  8')  
 Water velocity through the feed water heater ( $v$ ) is selected as 0.6 m/s.

$\tau_1 = x/v = 4.07$  s

$w$  is assumed to be approximetly 9.81 kN/m<sup>3</sup> (1000 kg<sub>f</sub>/m<sup>3</sup>).

1)  $n = \frac{\bar{G}}{\frac{\pi}{4} d_i^2 v w * 3600} \approx 56$  tubes

2) From steam tables:  
 Condenser saturation temperature 37.5 °C  
 $\Delta\theta_r = 39.03$  °C (based on equal temperature rise per heater).

Saturation temperature of steam = 37.5 + 39.03 + 2.78 = 79.31 °C

which corresponds to a pressure equals 46060 Pa (0.4606 bar)

Steam pressure in shell (P) is assumed to be 3/8 of the bled steam pressure = 17270 Pa

Hence, from steam tables  $\frac{\partial P}{\partial \theta_s} = 802$  Pa/K at shell pressure.

Dryness fraction of bled steam ( $\kappa$ ) in shell is assumed to be 0.88.

Specific volume of dry and saturated steam at shell pressure = 7.7303 m<sup>3</sup>/kg,  $\lambda = 2365.3227$  kJ/kg

3)  $LMTD = \frac{(79.31 - 37.5) - (79.31 - 76.53)}{\ln \frac{41.81}{2.78}} = 14.3945$  °C

4)  $UA = \frac{\bar{G} \times 4.187 \times \Delta\theta_r}{3600 \times LMTD} = 85.7727$  kJ/K.s

5)  $F_s = \frac{\bar{G} \times 4.187 \times \Delta\theta_r}{\lambda \times 3600} \approx 0.53$  kg/s

6) Vapour volume in shell =  $\frac{\pi}{4} [d_s^2 \cdot n - d_o^2] \cdot (x) \approx 0.4$  m<sup>3</sup>

7)  $M_v = \frac{0.4}{0.88 \times 7.7303} = 0.0592$  kg of steam

8)  $C_v = \frac{M_v}{P} \lambda \left( \frac{\partial P}{\partial \theta_s} \right) = 6.5027$  KJ/K

9) The specific heat of wall  $c_w = 0.3936$  KJ/ kg.K  
 $\rho_w = 8835$  kg/m<sup>3</sup>,  $C_w = \frac{\pi}{4} [d_o^2 - d_i^2] \cdot (x) \cdot n \cdot c_w \cdot \rho_w = 28.6926$  kJ/K

Table (1) Parameters Dependent Data

Boiler Load	100% (27200 kg/hr)				90% (24480 kg/hr)				110% (29920 kg/hr)			
FWT	115.5 °C (2 heaters)		160 °C (3 heaters)		115.5 °C (2 heaters)		160 °C (3 heaters)		115.5 °C (2 heaters)		160 °C (3 heaters)	
Vacuum bar abs.	0.0478	0.0647	0.0478	0.0647	0.0478	0.0647	0.0478	0.0647	0.0478	0.0647	0.0478	0.0647
Case No.	1	2	3	4	5	6	7	8	9	10	11	12
$\theta_b, ^\circ C$	79.31	81.81	81.10	84.44	79.31	81.81	81.10	84.44	79.31	81.81	81.10	84.44
$P_b, \text{bar}$	0.461	0.510	0.495	0.566	0.461	0.510	0.495	0.566	0.461	0.510	0.495	0.566
$\Delta\theta_r, ^\circ C$	39.03	36.43	40.83	39.17	39.03	36.43	40.83	39.17	39.03	36.43	40.83	39.17
$LMTD, ^\circ C$	14.40	13.78	14.83	14.43	14.40	13.78	14.83	14.43	14.40	13.78	14.83	14.43
$v, \text{m/s}$	0.60	0.60	0.60	0.60	0.54	0.54	0.54	0.54	0.66	0.66	0.66	0.66
$\tau_1, \text{s}$	4.07	4.07	4.07	4.07	4.52	4.52	4.52	4.52	3.70	3.70	3.70	3.70
U.A KJ/K.s	85.77	83.63	87.12	85.88	77.20	75.27	78.41	77.29	94.35	92.00	95.83	94.47
$F_s, \text{kg/s}$	0.53	0.50	0.55	0.53	0.48	0.45	0.50	0.48	0.58	0.54	0.61	0.59
$\lambda, \text{kJ/kg}$	2365.32	2360.05	2361.53	2354.51	2365.32	2360.05	2361.53	2354.51	2365.32	2360.05	2361.53	2354.51
$\frac{\partial P/\partial a_s}{Pa/k}$	802	905	869	980	802	905	869	980	802	905	869	980
$e_s, \text{kg/m}^3$	0.129	0.142	0.138	0.157	0.129	0.142	0.138	0.157	0.129	0.142	0.138	0.157
$M_v, \text{kg}$	0.059	0.057	0.056	0.063	0.059	0.057	0.056	0.063	0.059	0.057	0.056	0.063
$C_v, \text{kJ/k}$	6.503	6.404	6.156	6.865	6.503	6.404	6.156	6.865	6.503	6.404	6.156	6.865
$C, \text{kJ/k}$	173.88	173.78	173.53	174.24	173.88	173.78	173.53	174.24	173.88	173.78	173.53	174.24
$F_m, \text{kg/m.s}$	600	600	600	600	540	540	540	540	660	660	660	660
$h_1, \text{kJ/hr.m.K}$	17272.4	17272.4	17272.4	17272.4	15876.2	15876.2	15876.2	15876.2	18641.0	18641.0	18641.0	18641.0
$T_1, \text{s}$	3.7	3.7	3.7	3.7	4.02	4.02	4.02	4.02	3.423	3.423	3.423	3.423
$T_2, \text{s}$	0.4	0.4	0.4	0.4	0.398	0.398	0.398	0.398	0.4	0.4	0.4	0.4
$T_{12}, \text{s}$	0.82	0.82	0.82	0.82	0.896	0.896	0.896	0.896	0.763	0.763	0.763	0.763
$a_o, \text{s}^{-1}$	0.177	0.177	0.177	0.177	0.169	0.169	0.169	0.169	0.187	0.187	0.187	0.187

$$10) \rho_{sh} = 8005.3428 \text{ kg/m}^3$$

$$c_{sh} = 0.4606 \text{ kJ/kg.K}$$

$$C_{sh} = \pi (d_{so} - d_s) (x) \cdot \rho_{sh} \cdot c_{sh}$$

$$= 138.6841 \text{ kJ/K}$$

$$11) C = C_v + C_w + C_{sh} = 173.8794 \text{ kJ/K}$$

$$12) h_1 = 0.0144 c_f \frac{F_m^{0.8}}{d_i^{0.2}} \text{ (in F.P.S. System) [1]}$$

where:  $F_m$  is the mass flow rate in (lb/hr. ft<sup>2</sup>)

$$\text{Free area} = n \times \frac{\pi}{4} d_i^2 = 0.1355 \text{ ft}^2$$

$$F_m = \frac{27200 \times 2.204}{0.1355} = 442361.2751 \text{ lb/hr. ft}^2$$

$$\text{and } c_f = 1 \text{ Btu/lb}_m \cdot ^\circ\text{F}$$

$$\text{Then } h_1 = 0.0144 \times c_f \times \frac{(442361.2751)^{0.8}}{(0.666/12)^{0.2}}$$

$$= 843.5786 \text{ Btu/hr. ft}^2 \cdot ^\circ\text{F}$$

$$= 17272.4332 \text{ kJ/hr. m}^2 \cdot \text{K}$$

13) In order to determine  $h_2$  [30]:

$$h_2 = c_1 b_1 4\sqrt{r_1} / 4\sqrt{L \cdot \delta\theta} \text{ in M.K.S. system.}$$

For horizontal tubes

$$c_1 = 0.72, L = d_o = 0.01905 \text{ m}$$

From attached tabular form [30]:

$$\text{at } \delta\theta = 80 - 20 = 60 \text{ } ^\circ\text{C}$$

$$\text{Then; } 4\sqrt{r_1} = 4.85,$$

$$b_1 = 2070 \text{ and}$$

$$h_2 = 7565.5393 \text{ Kcal/m}^2 \cdot \text{hr.K}$$

$$= 31677 \text{ kJ/m}^2 \cdot \text{hr.K}$$

$$14) M_f = \frac{\pi}{4} d_i^2 \cdot \rho_f = 0.2248 \text{ kg/m length for one tube,}$$

$$A_1 = \pi \cdot d_i = 0.0532 \text{ m}^2/\text{m length for one tube,}$$

$$c_f = 4.187 \text{ kJ/kg.K then:}$$

$$T_1 = \frac{M_f \cdot c_f}{h_1 \cdot A_1} \times 3600 = 3.7 \text{ s}$$

$$15) M_w = \frac{\pi}{4} [d_o^2 - d_i^2] \cdot \rho_w$$

$$= 0.5319 \text{ kg/m length for one tube,}$$

$$A_2 = \pi d_o = 0.06 \text{ m}^2/\text{m length of one tube,}$$

then:

$$T_2 = \frac{M_w \cdot c_w}{h_2 \cdot A_2} \times 3600 = 0.4 \text{ s}$$

$$16) T_{12} = \frac{M_w \cdot c_w}{h_1 \cdot A_1} \times 3600 = 0.82 \text{ s}$$

$$17) a = \frac{(T_1 S + 1)(T_{12} T_2 S + T_{12} + T_2) - T_2}{T_1 (T_{12} T_2 S + T_{12} + T_2)}$$

$$= \frac{(3.7 S + 1)(0.82 \times 0.4 S + 0.82 + 0.4) - 0.4}{3.7(0.82 \times 0.4 S + 0.82 + 0.4)}$$

$$\approx S + 0.1772 \text{ 1/s}$$

$$18) e^{-a\tau_1} = e^{-(S+0.1772) 4.07} = 0.4861 e^{-4.07S}$$

$$19) \frac{b}{a} = \frac{1}{T_1 T_2 S^2 + (T_1 + T_2 + T_1 T_2 / T_{12}) S + 1}$$

$$= \frac{1}{1.48 S^2 + 5.9049 S + 1}$$

$$20) K_v = 0.05, K_p = 3.5 \text{ mm/K, } K = 0.4562, \tau = 0.3 \text{ s,}$$

$$\tau_v = 3 \text{ s, } \tau_d = 6 \text{ s}$$

$$\text{and } T = 1 \text{ s}$$

$$\text{Then, } \Theta.L.T.F = \frac{\sum_{i=0}^4 n_i S^i}{\sum_{j=0}^{10} m_j \cdot S^j}$$

where,

$$[n_0 \ n_1 \ \dots \ n_4] = [51.5389 \ 277.528 \ -76.2319 \ -10.2971 \ 5.9246]$$

and

$$[m_0 \ m_1 \ \dots \ m_{10}] = [63.7334 \ 1349.796 \ 11354.16 \ 48778.05 \ 115905.0 \ 157860.0 \ 127802.9 \ 60859.23 \ 16825.64 \ 2523.554 \ 159.809]$$

and C.L.T.F. = 
$$\frac{\sum_{i=0}^5 p_i S^i}{\sum_{j=0}^{10} q_j S^j}$$

where,

$$[p_0 \ p_1 \ \dots \ p_5] = [112.9681 \ 1399.0897 \ 4825.3955 \ 3119.5778 \ 813.0678 \ 77.9479]$$

and

$$[q_0 \ q_1 \ \dots \ q_{10}] = [115.2723 \ 1627.324 \ 11277.93 \ 48767.75 \ 115910.9 \ 157860.0 \ 127802.9 \ 60859.23 \ 16825.64 \ 2523.554 \ 159.809]$$